ICON in Climate Limited-area Mode (ICON Release Version 2.6.1): a new regional climate model

Trang Van Pham[1], Christian Steger[1], Burkhardt Rockel[2], Klaus Keuler[3], Ingo Kirchner[4], Mariano Mertens[5], Daniel Rieger[1], Günther Zängl[1], and Barbara Früh[1]

[1]Deutscher Wetterdienst, Frankfurterstr. 135, 63067 Offenbach am Main, Germany
[2]Helmholtz-Zentrum Geesthacht, Max-Planck-Str. 1, 21502 Geesthacht, Germany
[3]Brandenburg University of Technology, P.O. 10 13 44, 03013 Cottbus, Germany
[4]Freie Universität Berlin, Carl-Heinrich-Becker-Weg 6-10, 12165 Berlin, Germany
[5]Deutsches Zentrum für Luft- und Raumfahrt e.V., Münchener Strasse 20, Oberpfaffenhofen, 82234 Wessling, Germany

Correspondence: Trang Van Pham (trang.pham-van@dwd.de)

Abstract. For the first time the limited-area mode of the new weather and climate model ICON has been used for a continuous long-term regional climate simulation over Europe. Building upon ICON-LAM, ICON-CLM (ICON in Climate Limited-area Mode, hereafter ICON-CLM, available in ICON Release Version 2.6.1) is an adaptation for climate applications. A first version of ICON-CLM is now available and has already been integrated into a starter package (ICON-CLM_SP Version Beta1). The starter package provides users with a technical infrastructure that facilitates long-term simulations as well as model evaluation and test routines. ICON-CLM and ICON-CLM_SP were successfully installed and tested on two different computing systems. Test with different domain decompositions showed bit-identical results, and no systematic outstanding differences were found in the results with different model time steps. Comparison was done between ICON-CLM and COSMO-CLM (the recommended model configuration by the CLM-Community) performance. For that, an evaluation run with ERA-Interim boundary conditions was carried out with the setups similar to the COSMO-CLM recommended optimal setups. ICON-CLM results showed biases in the same range as those of COSMO-CLM for all evaluated surface variables. This is remarkable since the COSMO-CLM simulation was carried out with the latest model version which has been developed for two decades and was carefully tuned for climate simulations on the European domain. Furthermore, ICON-CLM already showed a better performance for air temperature, its daily extremes, and total cloud cover. Results for precipitation and mean sea level pressure did not show clear advantage from any model. However, as ICON-CLM is still in the early stage of development, there is still much room for improvement.

1 Background information

In 1999, the limited-area weather forecast model LM (Lokalmodell, Doms and Schättler (1999), later COSMO, Baldauf et al. (2011)), which was developed by the Deutscher Wetterdienst (DWD, the German Meteorological Service), went operational together with the global model GME (Majewski and Ritter, 2002). A few years later, it was renamed into "COSMO model" in order to reflect that further development has become a joint task of the COnsortium for Small scale MOdelling (COSMO). In

2002, CLM-Community developed the first version of the regional climate model named CLM. In 2007, the developments in COSMO and CLM were recombined and a first unified version of the weather forecast and climate modes, named COSMO-CLM (Rockel et al., 2008), was released.

In 2001, a cooperation between DWD and Max-Planck Institute for Meteorology (MPI-M) was initiated, with the aim
5   to develop a new modelling system for weather forecast and climate prediction. The new system was intended to replace the existing system COSMO/GME for operational weather forecast on one side and, on the other side, the global climate and earth system model ECHAM6/MPI-ESM (Stevens et al., 2013; Giorgetta et al., 2013). As a result of this initiative, the global numerical weather forecast model ICON (Icosahedral Nonhydrostatic) (Zängl et al., 2015) was developed and replaced GME as the operational model at DWD on the 20th of January 2015. As a next step, in December 2016, a domain with grid
10 refinement over Europe (ICON-EU-Nest) within the global ICON replaced the COSMO-EU for higher-resolution forecasts on the European domain. In the second half of 2020, the convection permitting configuration of ICON-LAM (ICON-D2) will replace the high resolution COSMO-D2 for the German domain and DWD will stop the operational use of the COSMO model after more than 20 years. This implies that the next unification of COSMO and COSMO-CLM (COSMO 6), scheduled for the end of 2019, will be the last one. Afterwards, the support for COSMO and COSMO-CLM will be gradually reduced.
15 In this work, we prepared state-of-the-art tools for climate applications for the upcoming years. Starting in 2017, DWD and the CLM-Community decided to develop a new regional climate model (ICON-CLM) based on the Limited-Area Mode of ICON (ICON-LAM). The preparation of ICON-CLM was triggered at DWD in the project ProWaS (Projection Service for Waterways and Shipping) – a joint pilot program of several German Federal Agencies – to prepare a regular federal forecasting and projection service about the influence of climate change on coastal and waterway traffic.
20 ICON can be used on a wide range of scales from climate prediction, numerical weather prediction (NWP) down to large-eddy simulations (Heinze et al., 2017). For these different scales, there is a number of different modes as shown in Figure 1. Generally there are three different physics packages available: the NWP, the ECHAM physics, and the large-eddy physics (which is not shown in Figure 1). The first one, named ICON-NWP, is used for operational weather forecasting at DWD. The second one, which is called ICON-A, originating from the ECHAM6 atmospheric model (Giorgetta et al., 2018), is used for
25 global climate simulations. This configuration is coupled to the global ocean model ICON-O (Korn, 2017) within the ICON Earth System Model (ICON-ESM). A feature for one- or two-way nested sub-domains with grid refinement is available in the NWP configuration and has recently also been transferred to ICON-A by DWD (ICON-EUClim). ICON-LAM denotes the limited-area mode of ICON, which currently is available for the NWP and large-eddy configurations. ICON-CLM builds upon ICON-LAM, and currently contains a set of technical adaptations for climate applications.
30 The aim of this paper is to introduce the new regional climate mode of ICON (ICON-CLM), along with its starter package ICON-CLM_SP, a supporting infrastructure needed to perform long-term simulations. Tests with different model time steps and tests on the impact of prescribing upper boundary conditions interpolated from re-analysis data were carried out. A long evaluation simulation driven by ERA-Interim re-analysis (Dee et al., 2011) was conducted over a period of 20 years and the results were compared to the evaluation simulation of the latest recommended COSMO-CLM version (CCLM 5.0 clm9). The
35 paper is structured as follows: The adaptations in model source code and technical infrastructure are described in Section

2. Section 3 gives details of the ICON-CLM model configuration and setup for the evaluation run as well as the evaluation methods we used. Results of this evaluation run in comparison to observational data and to the results of the latest COSMO-CLM version are shown in Section 4. Conclusions are provided in Section 5.

2 Model development

5   As the Limited-Area Mode of ICON, which ICON-CLM builds upon, has originally been developed for NWP applications, several adaptations and technical extensions were necessary to prepare the model for climate applications. Apart from the adjustments in the code, long-term climate simulations require a technical infrastructure for data and job management. Such an infrastructure has also been developed based on the existing infrastructure of COSMO-CLM.

2.1 The regional climate model ICON-CLM

10   Weather forecasting, which predicts the state of the atmosphere only up to about 2 weeks in advance, often does not involve the development of the ocean state. The ocean surface condition, hence, is often kept constant during the forecasts in weather prediction models or just slightly adjusted with a climatological trend for the forecast period. Thus, the sea surface temperature (SST) and sea-ice cover in ICON-LAM can only be updated monthly. For ICON-CLM, it is necessary to have a more frequent (up to hourly) update of SST and sea ice from external data. For this purpose, an option for higher update frequencies of these

15   boundary conditions was implemented in ICON-CLM. Time-dependent SST and sea-ice data can now be read from external data files and are fed to ICON-CLM with an user-defined interval (e.g. 1 hourly or 6 hourly). The user can select this option of frequent update of SST and sea ice via namelist settings. The external SST and sea ice data must be prepared and remapped to the ICON grid.

Similarly, the green house gas (GHG) values are usually kept constant in weather forecast models, because the changes

20   during the forecast period are negligible. In climate projections, however, it is necessary to use the time-dependent GHGs from climate change scenarios. Such an option was already available in ICON, but only in combination with the ECHAM physics package. The corresponding read routine was therefore extended so that it works for the NWP physics as well. Some additions to the NWP radiation scheme were made with respect to the GHG vertical profile with a new option to get the profile from external gas data. A file that contains yearly values of CO_2, CH_4, N_2O and Chlorofluorocarbons (CFC) for all years of the

25   experiment needs to be prepared in advance. These features of the time-dependent SST and GHG were largely based on the corresponding implementations in the ICON-A (Giorgetta et al., 2018).

For the upper boundary, ICON-LAM offers an option of prescribing the upper boundary conditions by using the same driving data source as for the lateral boundary conditions (nudging option). Users can define the height of the nudging zone as well as the nudging coefficients for the horizontal wind and for the thermodynamic variables via namelist settings. If this vertical

30   nudging option is turned off, a Rayleigh damping is applied to the vertical wind speed within the damping layer in order to prevent unphysical reflection of vertically propagating gravity waves.

In the NWP configuration of ICON-LAM, the number of soil layers is always constant with eight layers. The depths of half soil layers are also fixed at values between 5 mm and 14.5 m. However, for climate simulations in domains other than Europe (e.g. Africa, Asia) or to achieve better simulation of the soil variables for European domain, it is usually reasonable to adjust these soil parameters. Therefore, an option for a flexible number and depth of the soil layers has been implemented in the

5   ICON-CLM code.

The input/output of ICON-CLM has also been adjusted to have more flexibility. In NWP mode, the precipitation data are accumulated from the start of the forecast till the end without any reset. This is suitable for short weather forecasts, but for long climate simulations, this procedure is inconvenient and could, in the worst case, cause problems due to data imprecision. Furthermore, the maximum and minimum 2-m temperature values are calculated for 6 hourly intervals in NWP applications,

10 while for climate simulations the standard for these output variables is usually 24 hours. To control this flexibility extensions, new namelist parameters were introduced in ICON-CLM.

At the lateral boundaries, ICON-LAM requires, by default, information on cloud liquid water content and cloud ice water content from the global forcing data. These input fields are usually available if the ICON-CLM lateral boundary conditions are taken from reanalysis data like ERA-Interim. But if global climate projections are used as lateral boundary conditions, these

15 fields are usually not provided. Thus, the model code has been adjusted so that if cloud liquid water content and cloud ice content are not available in the lateral boundary data, these variables are initialized with zero.

Table 1 provides an overview of some differences between COSMO-CLM and ICON-CLM.

2.2   The starter package ICON-CLM_SP

In order to facilitate long-term climate simulations, we developed a run time infrastructure called starter package and a separate

20 evaluation tool. Both are provided along with the ICON-CLM model source code. The starter package ICON-CLM_SP contains a run routine, a climatological testsuite, all necessary utilities and configure scripts for different super computing environments. At the moment, two system settings for Cray (DWD) and Atos/Bull (DKRZ) are supported and tested. Settings for other machines could be easily added if necessary.

The run routine in ICON-CLM_SP, called "subchain", was adapted from the routine of the existing COSMO-CLM package.

25 The "subchain" contains five sub-routines for input preparation (prep), converting input data (conv2icon), ICON-CLM job management (icon), archiving (arch) and postprocessing (post) of the model output. Sub-routine "prep" copies and checks all the global forcing data as input for "conv2icon". Then "conv2icon" preprocesses and interpolates the initial data and the lateral, lower and upper boundary data onto the ICON-CLM model grid for the current model simulation. Sub-routine "icon" does the job management for ICON-CLM model. After that, all model output data are compressed by "arch" and some post-processing

30 steps like the provision of time series of selected output variables are done in "post".

A climatological testsuite (CTS) was also created based on the CTS from COSMO-CLM. In the CTS, 5-year test simulations can be done automatically with "subchain". The users can choose one simulation as a reference. The test simulations then will be compared with the reference simulation with respect to observational data (E-OBS and CRU, see Section 3.2 for more details) by an extra sub-routine called "eval". At the end, the results are visualized with standardized plots. This CTS was built

for the purpose of testing different versions of model source codes, or different setups of the same model version. Hence, it is a very helpful tool for model development and tuning.

Besides the sub-routine "eval" in CTS, a separate evaluation tool called "ETOOLS" was also adapted from the COSMO-CLM evaluation tool. This tool provides comparisons of the simulation results with observation data sets and creates standardized

5 plots to visualize the results. In order to facilitate the transition from COSMO-CLM to ICON-CLM for the users, both ICON-CLM_SP and ETOOLS were created such that the "look and feel" as well as the usage of the software packages is as similar as possible to the corresponding packages that exist for the COSMO-CLM model. The output structure of ICON-CLM or post-processed time series from "subchain/post" are also similar to those of COSMO-CLM for the same reason. Furthermore, users should be able to use all existing scripts and programs that were developed for COSMO-CLM output also for ICON-CLM

10 data.

3 Data and methods

3.1 Model configuration and experiment setup

After the implementation of the necessary changes in the model source code, a number of technical tests was performed. First, the influence of different domain decompositions for parallelization on the results were tested at the super computer at DWD

15 (Cray XC40). Results were binary identical, independent of the domain decomposition and the number of processors used for the simulations. Repeating tests starting from the same restart state were also carried out. ICON-CLM also showed binary identical results here.

All of the ICON-CLM tests described afterwards and the evaluation run were performed at the resolution R2B8 (approximately 10 km) on a domain completely covering the EU-CORDEX domain (Giorgi et al., 2009) (Figure 2, left). The model

20 atmosphere is divided into 70 layers and the model top is at a height of 30 km. The soil in ICON-CLM contains eight layers down to a depth of 14.5 m. ICON-CLM was driven at the lateral and lower boundaries by ERA-Interim at 6 hourly intervals. The model atmosphere was initialized with ERA-Interim data. The soil temperature and soil moisture were taken from a previous test simulation which is long enough to ensure that the spin-up of the soil has been completed. For the upper boundary, as described in Section 2, there are two options: (1) Using the driving data and nudging gradually in the relaxation zone; (2)

25 Damping the vertical wind beneath the upper boundary. To assess the impact of these two options, two 10-year simulations (1979-1988) were done with the same setups, with and without global data nudging. Analysis from these 10-year runs resulted in very minor differences on surface variables and none of the options showed any advantage over the other. For the evaluation run, we chose the option with nudging data at the upper boundary with ERA-Interim data, as later we wanted to compare the results with those from a COSMO-CLM run using a similar nudging option. The nudging zone started from the height of 12 km

30 to the model top of atmosphere (30 km).

In order to find a suitable model configuration for ICON-CLM at the resolution R2B8, an optimized namelist setup was used, namely the setup from ICON-LAM for R3B7 with nested domain on R3B8 grid (approximately 13 km and 6.5 km respectively). The tuning parameters were taken over from the global settings. In this setting, the Tiedke/Bechtold (Bechtold

et al., 2008) convection parameterization scheme and the Rapid Radiation Transfer Model (RRTM) radiation scheme (Mlawer et al., 1997) were used. These setups were checked to make sure that they are appropriate for climate applications and were used in all simulations. Former simulations (not published) with COSMO-CLM showed that in some cases the model results depend on the chosen model time steps. There is one particular time step that leads to larger biases in precipitation and surface pressure,

5 especially over the Alps and the south western area of the model domain. This issue has been analyzed by the CLM-Community but is still not fully understood yet. To ensure that such a dependency of the results on the model time step is not present in ICON-CLM, different fast physics/advection time step (hereafter: time step) choices were tested. At R2B8 (approximately 10 km) resolution, the time step should not exceed 120 seconds for stability reasons. With the common model and experiment setups described above, we carried out multiple one-year simulations for the year 1979 with time steps of 60, 80, 90, 100 and

10 120 seconds. Figure 3 shows the biases compared to reference data of 2-m temperature, mean sea level pressure (MSLP), total precipitation and total cloud cover. The biases were averaged for each month and for the Alpine region (sub-region denoted AL in Figure 2, right). Colors show the different time step experiments. The biases for all variables from any particular time-step experiment were small and did not stand out from the rest. The results were similar for all sub-regions shown in Figure 2 (right) and therefore are not shown here. The annual and seasonal biases of these multiple one-year simulations were also very similar

15 in all cases (not shown here).

Because there is no big difference in the model results depending on the choice of time step, for experiments at spatial resolution R2B8, we chose the time step of 90 seconds due to the computational efficiency and stability. An evaluation run was carried out for the EU-CORDEX domain at the resolution R2B8. The simulation period is 1979 to 2000. The model and experiment setups were the common setups as described above, this evaluation run is later referred to as ICLM-REF.

20 The results of ICLM-REF were compared to the reference experiment of the recent recommended version of COSMO-CLM (v5.0_clm9). This COSMO-CLM simulation is later referred to as CCLM-REF. This COSMO-CLM setup showed the best performance for the European domain in an inter-comparison with several other setups which was performed within the COPAT (COordinated Parameter Tuning) project in the CLM-Community. The simulation period is 1979 to 2000. The initial, lower and lateral boundary data are taken from ERA-Interim. A sponge layer with Rayleigh damping in the upper levels of

25 COSMO-CLM domain was used. The damping was done against the external boundary values, similarly to the nudging at the model top in ICLM-REF simulation and thus the results from both experiments are comparable.

3.2 Evaluation methods

For model assessment and evaluation, output fields from six variables were analyzed, namely 2-m temperature, daily maximum and minimum values of 2-m temperature, MSLP, total precipitation and total cloud cover. Monthly average values of these vari-

30 ables were calculated and used for further analysis. For total precipitation, the monthly accumulated amounts were calculated. Parts of the evaluation were carried out based on seasonal averages. The following definitions and abbreviations of the seasons are used in this paper: winter - December, January, February (DJF), spring - March, April, May (MAM), summer - June, July, August (JJA), and autumn - September, October, November (SON). Results were averaged for eights sub-regions as already used in the PRUDENCE projects (described by Christensen and Christensen (2007)). These sub-regions are: Britian Iles (BI),

Iberian Peninsula (IP), France (FR), Mid-Europe (ME), Scandinavia (SC), Alps (AL), Mediterranean (MD) and Eastern Europe (EA) (shown on Figure 2, right).

For the evaluation of monthly mean values of 2-m temperature, daily maximum and minimum 2-m temperature, MSLP and total precipitation, the E-OBS dataset (Haylock et al., 2008; Van den Besselaar et al., 2011) was used as reference data.

5 E-OBS is a 0.25° gridded daily dataset covering all of Europe. The data are available over land and available from quite recent back to 1950. In order to compare 2-m temperature data from different datasets (ICON-CLM, COSMO-CLM and E-OBS), a height correction was performed. The model temperature values at E-OBS 2-m height were calculated based on the differences between model and E-OBS surface elevation and the moist adiabatic lapse rate (0.0065K/m). The reference cloud data, which was used for assessment of the model cloud cover, are CRU TS data (Harris et al., 2014). This is a monthly gridded dataset

10 at 0.5° resolution, available globally over land area. The dataset covers the period from 1901 to 2013. Because the outputs of ICLM-REF and CCLM-REF were written on rotated grids that are finer than E-OBS and CRU grids, these data were transformed to the lat-lon grids of the observational data or the purpose of comparison.

The evaluation within COPAT for 2-m temperature, MSLP and cloud cover was done using E-OBS version 10.0 and CRU version 3.22 as reference data. Therefore, in order to compare our evaluation to the one from COPAT, we also used the same

15 versions of the data sets. The comparison period is 20 years from 1981 to 2000, the same as the evaluation period in COPAT. The reference total precipitation data was taken from E-OBS version 12.0 because this dataset (among versions from 10.0 to 17.0) shows the fewest missing data for precipitation over the area of Poland.

Some important climate indices (listed in Table 2) were calculated from ICON-CLM, COSMO-CLM and E-OBS 2-m temperature and total precipitation data for the entire period 1981-2000. The number of days that fulfils the definition (in Table

20 2) was counted for each horizontal grid cell, then averaged over a sub-region.

Root-mean-square error (RMSE) was calculated from the model and observed monthly values:

$$RMSE = \sqrt{\frac{1}{N}\sum_{i=1}^{n}(S_i - O_i)^2} \tag{1}$$

where S_i and O_i are the model (ICLM-REF or CCLM-REF) and E-OBS monthly values, respectively, averaged over the sub-regions considered at the ith month; N is the total number of months in the evaluation period 1981-2000. To compare the

25 spatial variability of the data, spatio-temporal standard deviation (STDEV) was also calculated from monthly fields of model and observed data for all simulation months, and then averaged over time.

4 Evaluation and comparison with COSMO-CLM

In the evaluation run, ICLM-REF showed a very good performance. In comparison with reference data, ICLM-REF biases are already of similar magnitude as the CCLM-REF biases. This result is consistent for all six evaluated variables and for all

30 PRUDENCE sub-regions. For certain areas or certain variables, ICLM-REF showed even smaller biases than CCLM-REF.

4.1 Air temperature

The 2-m temperature bias of ICLM-REF and CCLM-REF was mostly within -1.5 K to 1.5 K relative to E-OBS data. Figure 4 shows the mean annual biases against E-OBS data over the 20 year period from 1981 to 2000 for ICLM-REF and CCLM-REF data for the entire domain. Biases over central Europe, especially Southern Germany and the Alps, from both experiments

5 were of the same sign, with smaller biases coming from ICLM-REF. ICLM-REF had a warm bias in most parts of Sweden and southern Russia, while CCLM-REF showed a cold bias in these regions. The Balkan region is well known for large air temperature biases in COSMO-CLM simulations (Anders and Rockel, 2009; Pham et al., 2014; Trusilova et al., 2014); which also occur in ICLM-REF with values up to +1.5 K.

The seasonal temperature bias in Figure 5 shows that the median of the bias in the sub-regions ranged from -0.6 K to 0.05 K

10 for ICLM-REF and -1.1 K to -0.3 K for CCLM-REF. While in many of the sub-regions and seasons nearly no bias was found for ICLM-REF (bias median in the order of 0.01 K), CCLM-REF had usually larger biases. Both models had smaller biases in winter and autumn and larger biases in spring and summer. Besides some sub-regions like Britain, Mid-Europe, France, Iberian Peninsula where small biases were found (especially from ICLM-REF), sub-regions Scandinavia, Alps, Mediterranean and Eastern Europe showed larger biases. The latter sub-regions also showed larger variability of biases in space, with the

15 bias range from -3.7 K to 3.4 K. CCLM-REF had almost always more variability in temperature bias than ICLM-REF. The differences in spatial variability in CCLM-REF were exceptionally strong in Scandinavia in winter and summer.

For extreme daily temperature bias, CCLM-REF and ICLM-REF showed opposite trends. CCLM-REF tended to underestimate the maximum 2-m temperature, while ICLM-REF overestimated the values. This can most clearly be seen in winter and autumn (Figure 6), where the medians of all ICLM-REF biases are positive and of all CCLM-REF biases are negative.

20 ICLM-REF clearly had smaller median biases ranging from -0.02 to 1 K (with one exception of 2.3 K), while the range in CCLM-REF was -2.5 to 1.2 K. In summer, the bias was larger for both models. CCLM-REF had larger spatial differences among the sub-regions than ICLM-REF. Similarly, ICLM-REF simulated the minimum 2-m temperature better than CCLM-REF with median biases ranging from -1.2 K to 0.5 K compared to -0.6 K and 1.8 K in CCLM-REF (Figure 7). ICLM-REF slightly underestimated the daily minimum 2-m temperature while CCLM-REF overestimated it. Consequently, the daily tem-

25 perature range was overestimated by ICLM-REF and underestimated by CCLM-REF. However, the representation of the daily temperature range is, in general, in ICLM-REF closer to the observed values than in CCLM-REF.

ICLM-REF had also smaller RMSE than CCLM-REF for 2-m temperature over most sub-regions with one exception in sub-region Iberian Peninsula (Table 3). RMSEs of ICLM-REF were all smaller than 0.9 K, whereas CCLM-REF had RMSE up to 1.03 K. Looking at the STDEV, CCLM-REF tended to overestimate the spatial variability. This can be most clearly seen in

30 sub-region Eastern Europe with STDEV of 9.03, 8.46 and 8.22 from CCLM-REF, ICLM-REF and E-OBS, respectively. ICLM-REF STDEV were closer to the E-OBS values than CCLM-REF STDEV in all sub-regions. The differences were especially pronounced in sub-regions Iberian Peninsula and France.

Similar results were found for minimum 2-m temperature, with ICLM-REF´s RMSEs and STDEVs closer to the values of E-OBS for all sub-regions (Table 5). Regarding RMSEs of maximum 2-m temperature (Table 4), in four out of eight sub-regions,

ICLM-REF got lower errors and seven sub-regions showed better spatial variation. Overall, ICLM-REF simulated average and daily extreme values of 2m air temperature better than CCLM-REF.

The better representation of daily extreme temperatures in ICLM-REF resulted in a better performance for climate indices that are determined by air temperature. Among those indices, CCLM-REF overestimated the total numbers of ice days and

5 tropical nights over the whole evaluation period (1981-2000) as can be seen in Figure 11. Largest tropical night overestimation was found for the sub-region Eastern Europe with 104 nights by CCLM-REF, 6.5 times more than that of E-OBS (16 nights), while the ICLM-REF result was much closer to the observations with only 23 nights. Beside that, ICLM-REF results were very close to the observed numbers for sub-regions France, Alps, Mediterranean, while the numbers in CCLM-REF clearly stand out against the observations. The results for the ice days index is similar. CCLM-REF overestimated the number of

10 ice days for all sub-regions. ICLM-REF, on the other hand, slightly underestimated the numbers of ice days but was in all regions much closer to the number derived from E-OBS than CCLM-REF. The representation of frost days was much better in CCLM-REF compared to the previous two indices, but ICLM-REF still showed a better performance than CCLM-REF in all eight sub-regions. Both models produced fewer frost days than observed, except for sub-region Scandinavia. The number of summer days was overestimated by ICLM-REF for six of the eight sub-regions, while CCLM-REF mostly underestimated the

15 amount of summer days. On average, for whole Europe, ICLM-REF resulted in 1065 summer days; the numbers from E-OBS and CCLM-REF are 1128 and 874, respectively.

4.2 Precipitation

The mean annual precipitation bias ranged from -50 mm/month to 50 mm/month in both models (Figure 4). Overall, both models simulated more precipitation than E-OBS data. However, one should keep in mind that E-OBS precipitation data tend

20 to give too low values. That might be the reason why both ICLM-REF and CCLM-REF overestimated precipitation in large part of the domain. CCLM-REF tended to produce too little precipitation than E-OBS along the Atlantic coast while ICLM-REF performed better in this area. In the western part of Germany, ICLM-REF had only a slight bias with a difference of less than 5 mm/month compared with the reference data. CCLM-REF, on the other hand, produced negative biases up to -20 mm/month in this area. However, over the eastern part of Germany, ICLM-REF had larger biases up to 10 mm/month. In all other regions,

25 the spatial distribution of precipitation biases was similar in both models.

Looking at the spatial variability of the seasonal biases within the sub-regions in Figure 8, we see that although for some sub-regions in certain seasons, the bias medians were close to zero, the ranges of biases were large. This is expected because precipitation is a highly inhomogeneous variable. Summer and autumn tended to have small median bias in ICLM-REF and CCLM-REF. Among the four seasons, summer had the smallest variation. For winter, summer and autumn, it is not clear which

30 model performed better. For spring, the median and the range of the bias were better in CCLM-REF compared to ICLM-REF for most of the sub-regions.

RMSEs of CCLM-REF were smaller than those of ICLM-REF for most of the sub-regions, except for sub-region Iberian Peninsula (Table 6). The spatial variability of precipitation in CCLM-REF was also closer to observations with better STDEV for five out of eight sub-regions.

ICLM-REF tended to have more precipitation days than CCLM-REF, with the wet days index higher for most of the sub-regions and only one exception for sub-region Scandinavia (Figure 11). ICLM-REF also produced more days with heavy and very heavy precipitation than CCLM-REF. For most of the sub-regions, both models overestimated heavy and very heavy precipitation indices. From our results, it is difficult to judge which model performed better for precipitation and precipitation

5 related climate indices. The results depended on the area as well as the season and the index (heavy/very heavy precipitation) considered.

4.3 MSLP and cloud cover

The bias of MSLP of the two models showed opposite signs. ICLM-REF had positive biases while the biases in CCLM-REF were mostly negative as revealed in Figure 4. Although both models had absolute biases up to 2.5 hPa, the performance of

10 CCLM-REF was better for the sub-regions Scandinavia and Iberian Peninsula. The opposite signs of the bias in the two model experiments can also be seen very clearly on Figure 10. Spring and autumn showed less spatial variability of MSLP values in both models. The representation of MSLP was in winter and autumn slightly better in CCLM-REF than in ICLM-REF with smaller median bias and smaller bias ranges. The RMSEs and STDEVs for MSLP are shown in Table 7. ICLM-REF had better RMSE than CCLM-REF in half of the sub-regions. However, ICLM-REF had some large errors over sub-regions Iberian

15 Peninsula and France with RMSEs of 1.9 hPa and 1.7 hPa, respectively. The performance of both models was very similar regarding the spatial variation of MSLP.

The representation of annual mean cloud cover in ICLM-REF looks much better than in CCLM-REF in Figure 4. CCLM-REF produced too much cloud cover over the sub-region Scandinavia and over the eastern part of the domain (up to 20% more cloud cover than CRU TS data). ICLM-REF, on the other hand, had biases of only up to +/- 10%. For most regions, the bias

20 was in the range of +/- 5%. The overestimation of cloud cover in the sub-regions Scandinavia and Eastern Europe might be the reason for the cold bias of CCLM-REF in these regions. On a seasonal mean, however, CCLM-REF showed a smaller negative bias during winter in all sub-regions (except Scandinavia), and its performance in autumn was comparable to ICLM-REF. The RMSEs and STDEVs of cloud cover did not show much difference between the two models. No concrete conclusion could be drawn from those numbers, therefore they were not shown here.

25 ## 5   Conclusions

The new regional climate model ICON-CLM has been derived from the weather forecast model ICON-LAM along with the necessary technical infrastructure allowing users to carry out long-term regional climate simulations. An evaluation run from the very first version of ICON-CLM showed very promising results. The ICON-CLM results were proven to be independent of the domain decomposition, and restarting with the same configuration gave binary identical results. In contrast to some

30 versions of to COSMO-CLM, ICON-CLM did not show any systematic dependency of the results on integration time steps. All tested time steps showed similar results with no bias outliers for any of the chosen values. These time step tests were done

with model horizontal resolution R2B8 (about 10 km) over the EU-CORDEX domain. When choosing another model grid spacing or simulating another domain, tests might be required to affirm these results.

The vertical nudging of the global forcing data at the model upper boundary did not show any notable impact on the climatology of surface variables. This is probably due to the fact that in our settings of ICON-CLM, the top of the atmosphere

5 was at 30 km height. When choosing a lower model top, one might see larger effects of the vertical nudging. Furthermore, in this study, we focused on the near-surface climate and therefore did not look at the upper air layers where larger differences between nudging and no nudging are can be found.

Results from the evaluation run showed that ICON-CLM performed already as well as COSMO-CLM. Especially for air temperature and temperature-related climate indices, improvements are visible in the ICLM-REF simulation. The reason might

10 be that ICON-CLM simulated better cloud cover with less overestimation over the northern and eastern part of the domain than COSMO-CLM. For precipitation and MSLP, the performance of both models was very similar. It should be taken into account that ICON-CLM is still in the early stage of development while COSMO-CLM has been developed and applied for NWP and climate applications for more than 20 years and was well-tuned with a large number of tested namelist combinations in the COPAT project. Therefore, ICON-CLM has still great potential to improve the model setup and with growing experience we

15 expect that ICON-CLM results will improve further in the upcoming years.

The next step in the ICON-CLM preparation will be a thorough model tuning by testing the sensitivity of the model to a variety of namelist parameters and their different combinations of namelist settings in order to find an optimal configuration. Climate simulations on different domains, e.g. CORDEX Africa, will be done to evaluate the ability of ICON-CLM to simulate different climates. So far only re-analysis driven simulation have been performed with ICON-CLM, but historical simulations

20 driven by the results of global climate simulations will also be done to test the model performance for this experiment type. Based on a well-evaluated model configuration, regional climate projections will be performed in order to address the impact of climate change at regional scale. Thus, climate projections, e.g. in the framework of CORDEX, will also be provided with ICON-CLM in the future. We plan to further develop ICON with the aim of unifying the different physics packages currently existing for the numerical weather prediction and the climate mode in order to pursue a "Seamless prediction" system with one

25 forecasting system which can produce produce forecasts and projections for all time-scales from weather prediction to seasonal and decadal predictions and climate projections.

Code availability. To institutions, the ICON model is distributed under an institutional license issued by DWD. In case of the institutional license, two copies of the institutional license need to be signed and returned to the DWD. The ICON Release Version 2.6.1 can be then downloaded at https://data.dwd.de.

30 To individuals, the ICON Model is distributed under a personal non-commercial research license distributed by MPI-M. Every person receiving a copy of the ICON framework code accepts the ICON personal-non-commercial research license by doing so. Or, as the license states: Any use of the ICON-Software is conditional upon and therefore leads to an implied acceptance of the terms of the Software License Agreement. To receive an individually licensed copy, please follow the instructions provided at https://code.mpimet.mpg.de/projects/iconpublic/wiki/Instructions_to_obtain_the_ICON_model_code_with_a_personal_non-commercial_research_license. The ICON Release Ver-

sion 2.6.1 model code with a personal non-commercial research license can be obtained at https://code.mpimet.mpg.de/projects/icon-downloads/files.

The starter package ICON-CLM_SP_beta1 can be downloaded from http://doi.org/10.5281/zenodo.3896136. The starter package will be shipped with a recommended configuration for EURO-CORDEX domain at the resolution R2B8 and will be available for all CLM-
5   Community members.

The forcing data were used for our simulations are the ERA-Interim data (Dee et al., 2011). Model evaluation was done againt E-OBS version 10.0 and 12.0 (Haylock et al., 2008; Van den Besselaar et al., 2011) und CRU TS version 3.22 datasets (Harris et al., 2014).

Appendix A

A1

10   *Author contributions.* Trang Van Pham implemented the adaptations in model code and ICON-CLM Starter Package, carried out the experiments and prepared the manuscripts with contributions from all co-authors. Christian Steger contributed in the organization and supervision of the work. Ingo Kirchner and Mariano Mertens are the source code administrators of ICON-CLM. Burkhardt Rockel contributed to the ICON-CLM Starter Package. Klaus Keuler, Burkhardt Rockel and Barbara Früh defined the research goals, aims and methodology. Daniel Rieger and Günther Zängl contributed in the development of ICON-NWP, the foundation for ICON-CLM.

15   *Competing interests.* The authors declare that they have no conflict of interest.

Disclaimer. TEXT

References

Anders, I. and Rockel, B.: The influence of prescribed soil type distribution on the representation of present climate in a regional climate model, Climate Dynam., 33, 177–186, 2009.

Baldauf, M., Seifert, A., Förstner, J., Majewski, D., Raschendorfer, M., and Reinhardt, T.: Operational convective-scale numerical weather prediction with the COSMO model: description and sensitivities, Monthly Weather Review, 139, 3887–3905, 2011.

Barker, H. W., Stephens, G., Partain, P., Bergman, J., Bonnel, B., Campana, K., Clothiaux, E., Clough, S., Cusack, S., Delamere, J., et al.: Assessing 1D atmospheric solar radiative transfer models: Interpretation and handling of unresolved clouds, Journal of Climate, 16, 2676–2699, 2003.

Bechtold, P., Köhler, M., Jung, T., Doblas-Reyes, F., Leutbecher, M., Rodwell, M. J., Vitart, F., and Balsamo, G.: Advances in simulating atmospheric variability with the ECMWF model: From synoptic to decadal time-scales, Quarterly Journal of the Royal Meteorological Society: A journal of the atmospheric sciences, applied meteorology and physical oceanography, 134, 1337–1351, 2008.

Christensen, J. H. and Christensen, O. B.: A summary of the PRUDENCE model projections of changes in European climate by the end of this century, Climatic change, 81, 7–30, 2007.

Dee, D. P., Uppala, S. M., Simmons, A. J., Berrisford, P., Poli, P., Kobayashi, S., Andrae, U., Balmaseda, M., Balsamo, G., Bauer, P., et al.: The ERA-Interim reanalysis: Configuration and performance of the data assimilation system, Q. J. R. Meteorol. Soc., 137, 553–597, https://doi.org/10.1002/qj.828, 2011.

Doms, G. and Schättler, U.: The nonhydrostatic limited-area model LM (Lokal-Modell) of DWD, Part I: Scientific documentation, Deutscher Wetterdienst (DWD), 10, 1999.

Doms, G., Förstner, J., Heise, E., Herzog, H., Mironov, D., Raschendorfer, M., Reinhardt, T., Ritter, B., Schrodin, R., Schulz, J.-P., et al.: A description of the nonhydrostatic regional COSMO model. Part II: Physical parameterization, Deutscher Wetterdienst, Offenbach, Germany, 2011.

Gal-Chen, T. and Somerville, R. C.: On the use of a coordinate transformation for the solution of the Navier-Stokes equations, Journal of Computational Physics, 17, 209–228, 1975.

Giorgetta, M. A., Jungclaus, J., Reick, C. H., Legutke, S., Bader, J., Böttinger, M., Brovkin, V., Crueger, T., Esch, M., Fieg, K., et al.: Climate and carbon cycle changes from 1850 to 2100 in MPI-ESM simulations for the Coupled Model Intercomparison Project phase 5, Journal of Advances in Modeling Earth Systems, 5, 572–597, 2013.

Giorgetta, M. A., Brokopf, R., Crueger, T., Esch, M., Fiedler, S., Helmert, J., Hohenegger, C., Kornblueh, L., Köhler, M., Manzini, E., et al.: ICON-A, the atmosphere component of the ICON Earth System Model. Part I: Model Description, Journal of Advances in Modeling Earth Systems, 2018.

Giorgi, F., Jones, C., Asrar, G. R., et al.: Addressing climate information needs at the regional level: the CORDEX framework, World Meteorological Organization (WMO) Bulletin, 58, 175, 2009.

Harris, I., Jones, P. D., Osborn, T. J., and Lister, D. H.: Updated high-resolution grids of monthly climatic observations–the CRU TS3. 10 Dataset, International journal of climatology, 34, 623–642, 2014.

Haylock, M., Hofstra, N., Klein Tank, A., Klok, E., Jones, P., and New, M.: A European daily high-resolution gridded data set of surface temperature and precipitation for 1950–2006, J. Geophys. Res.: Atmospheres, 113, https://doi.org/10.1029/2008JD10201, 2008.

Heinze, R., Dipankar, A., Henken, C. C., Moseley, C., Sourdeval, O., Trömel, S., Xie, X., Adamidis, P., Ament, F., Baars, H., et al.: Large-eddy simulations over Germany using ICON: A comprehensive evaluation, Quarterly Journal of the Royal Meteorological Society, 143, 69–100, 2017.

Korn, P.: Formulation of an unstructured grid model for global ocean dynamics, Journal of Computational Physics, 339, 525–552, 2017.

5 Majewski, D. and Ritter, B.: Das Global-Modell GME, Promet, 27, 111–122, 2002.

Mlawer, E. J., Taubman, S. J., Brown, P. D., Iacono, M. J., and Clough, S. A.: Radiative transfer for inhomogeneous atmospheres: RRTM, a validated correlated-k model for the longwave, Journal of Geophysical Research: Atmospheres, 102, 16 663–16 682, 1997.

Orr, A., Bechtold, P., Scinocca, J., Ern, M., and Janiskova, M.: Improved middle atmosphere climate and forecasts in the ECMWF model through a nonorographic gravity wave drag parameterization, Journal of Climate, 23, 5905–5926, 2010.

10 Pham, T. V., Brauch, J., Dieterich, C., Früh, B., and Ahrens, B.: New coupled atmosphere-ocean-ice system COSMO-CLM/NEMO: assessing air temperature sensitivity over the North and Baltic Seas, Oceanologia, 56, 167–189, https://doi.org/10.5697/oc.56-2.167, 2014.

Ritter, B. and Geleyn, J.-F.: A comprehensive radiation scheme for numerical weather prediction models with potential applications in climate simulations, Monthly Weather Review, 120, 303–325, 1992.

Rockel, B., Will, A., and Hense, A.: The regional climate model COSMO-CLM (CCLM), Meteorol. Z., 17, 347–348, https://doi.org/10.1127/0941-2948/2008/0309, 2008.

15 Schär, C., Leuenberger, D., Fuhrer, O., Lüthi, D., and Girard, C.: A new terrain-following vertical coordinate formulation for atmospheric prediction models, Monthly Weather Review, 130, 2459–2480, 2002.

Schrodin, R. and Heise, E.: The multi-layer version of the DWD soil model TERRA_LM, DWD, 2001.

Schulz, J.-P., Vogel, G., Becker, C., Kothe, S., Rummel, U., and Ahrens, B.: Evaluation of the ground heat flux simulated by a multi-layer land surface scheme using high-quality observations at grass land and bare soil, Meteorologische Zeitschrift, 25, 607–620, https://doi.org/10.1127/metz/2016/0537, http://dx.doi.org/10.1127/metz/2016/0537, 2016.

Seifert, A. and Beheng, K. D.: A double-moment parameterization for simulating autoconversion, accretion and selfcollection, Atmospheric research, 59, 265–281, 2001.

Stevens, B., Giorgetta, M., Esch, M., Mauritsen, T., Crueger, T., Rast, S., Salzmann, M., Schmidt, H., Bader, J., Block, K., et al.: Atmospheric component of the MPI-M Earth System Model: ECHAM6, J. Adv. Model Earth Syst., 5, 146–172, https://doi.org/10.1002/jame.20015, 2013.

Tiedtke, M.: A comprehensive mass flux scheme for cumulus parameterization in large-scale models, Monthly Weather Review, 117, 1779–1800, 1989.

Trusilova, K., Früh, B., Brienen, S., and Keuler, K.: Urban effects in climate simulations for CORDEX Europe, CLM-Community Newsletter, 2, 4–7, 2014.

Van den Besselaar, E., Haylock, M., Van der Schrier, G., and Klein Tank, A.: A European daily high-resolution observational gridded data set of sea level pressure, Journal of Geophysical Research: Atmospheres, 116, 2011.

Zängl, G., Reinert, D., Rípodas, P., and Baldauf, M.: The ICON (ICOsahedral Non-hydrostatic) modelling framework of DWD and MPI-M: Description of the non-hydrostatic dynamical core, Quarterly Journal of the Royal Meteorological Society, 141, 563–579, https://doi.org/https://doi.org/10.1002/qj.2378, 2015.
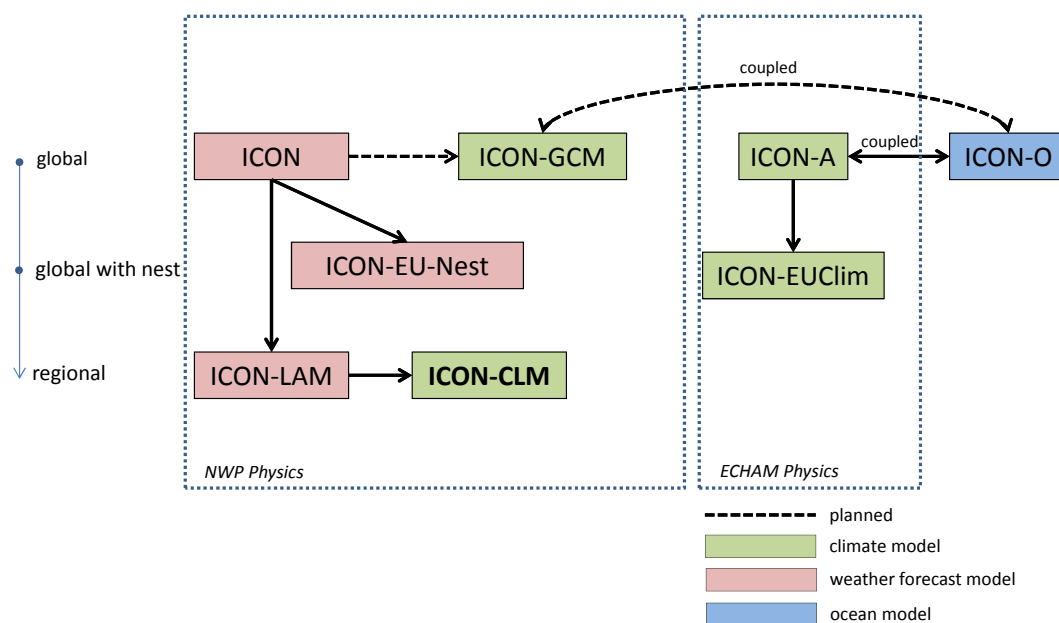
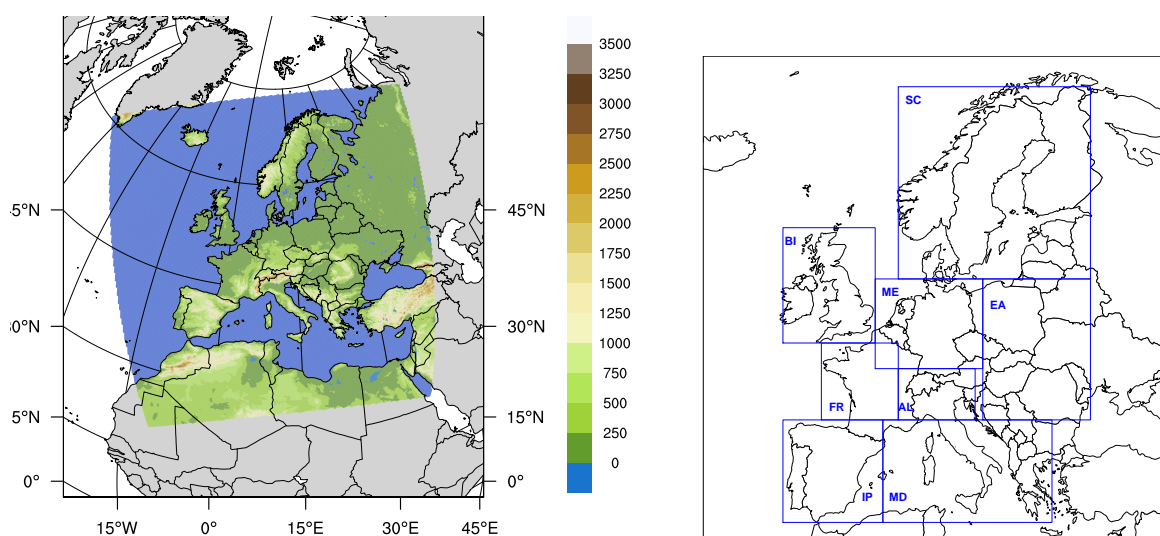**Figure 1.** Overview ICON modelling framework.

Figure 2. Simulation domain EU-CORDEX and model orography [m] of ICLM-REF on the R2B8 grid (left). Evaluation was done for the eight PRUDENCE sub-regions (right).
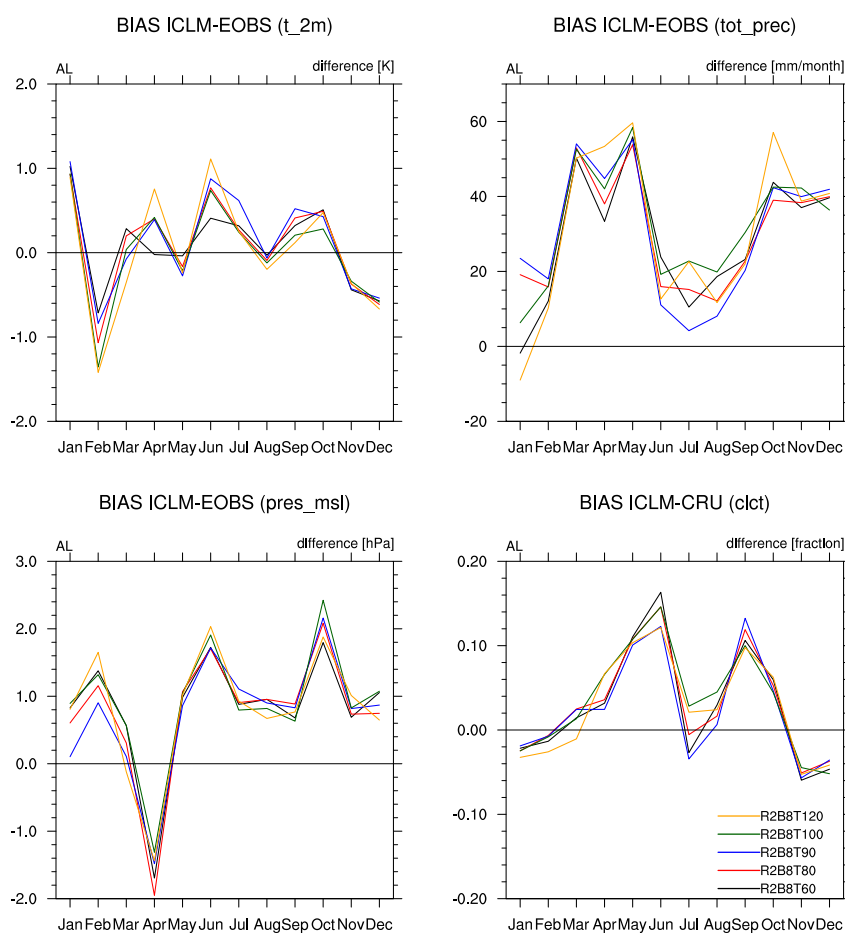
Figure 3. Monthly averaged biases of 2-m temperature, total precipitation, MSLP for different model time steps compared to E-OBS data and total cloud cover compared with CRU TS data. Data were averaged for the Alpine region and for year 1979.
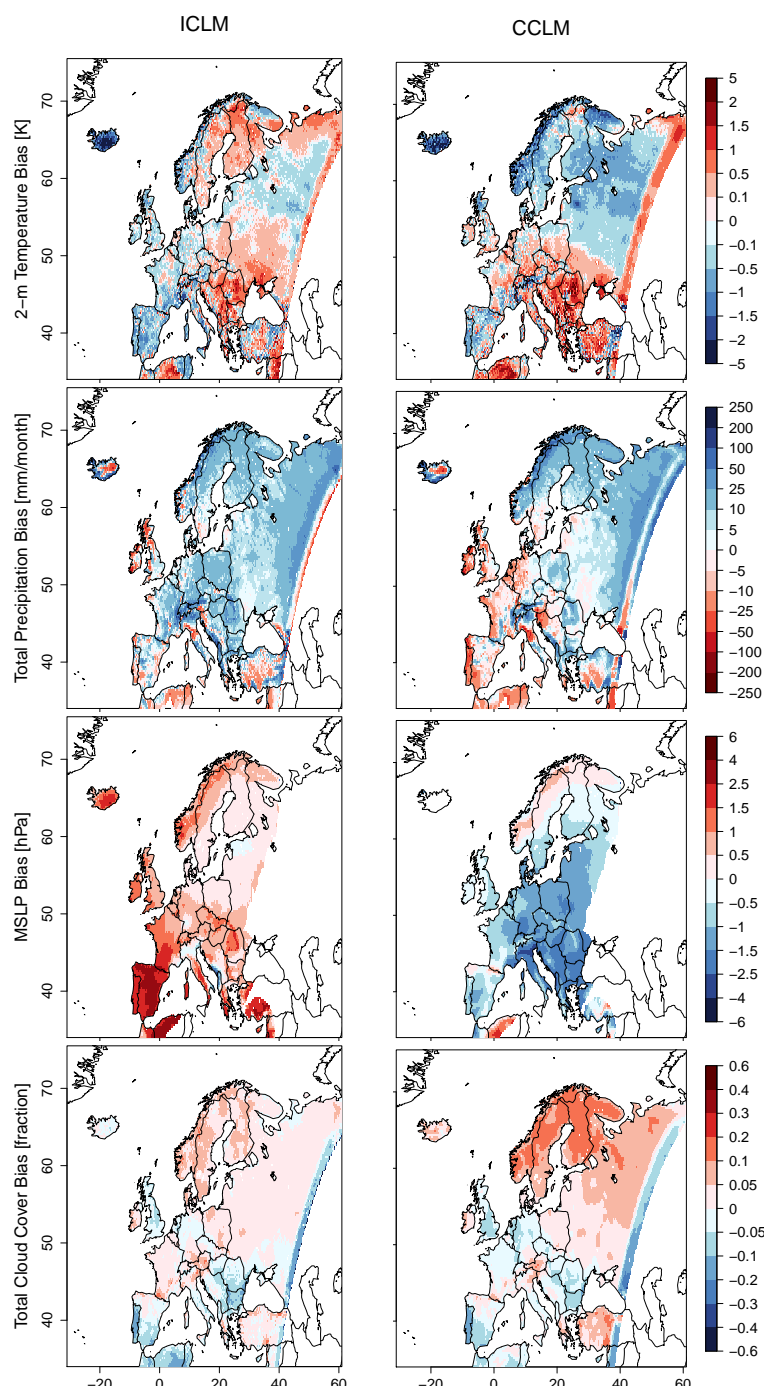
Figure 4. Multi-year averaged biases against E-OBS 10.0 and CRU TS 3.22 data for the period 1981-2000 for 2-m temperature, total precipitation, MSLP and total cloud cover (from top to bottom respectively) from ICON-CLM and COSMO-CLM evaluation runs (left and right respectively).
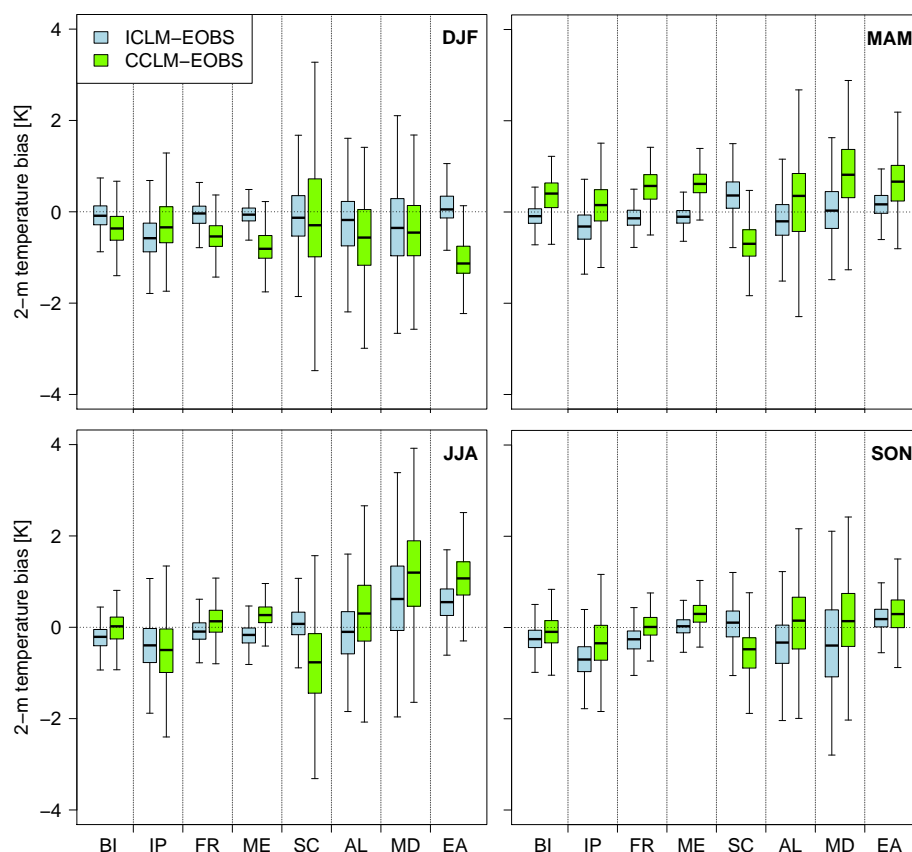
Figure 5. Seasonal mean 2-m temperature biases of ICON-CLM and COSMO-CLM data against E-OBS data for all PRUDENCE sub-regions. Values averaged for the period 1981 to 2000. Spatial variability within a sub-region is indicated by the lower bar (5th), upper bar (95th), lower edge of the box (25th), middle of the box (50th) and upper edge of the box (75th percentile of the distribution of all grid points within a sub-region).

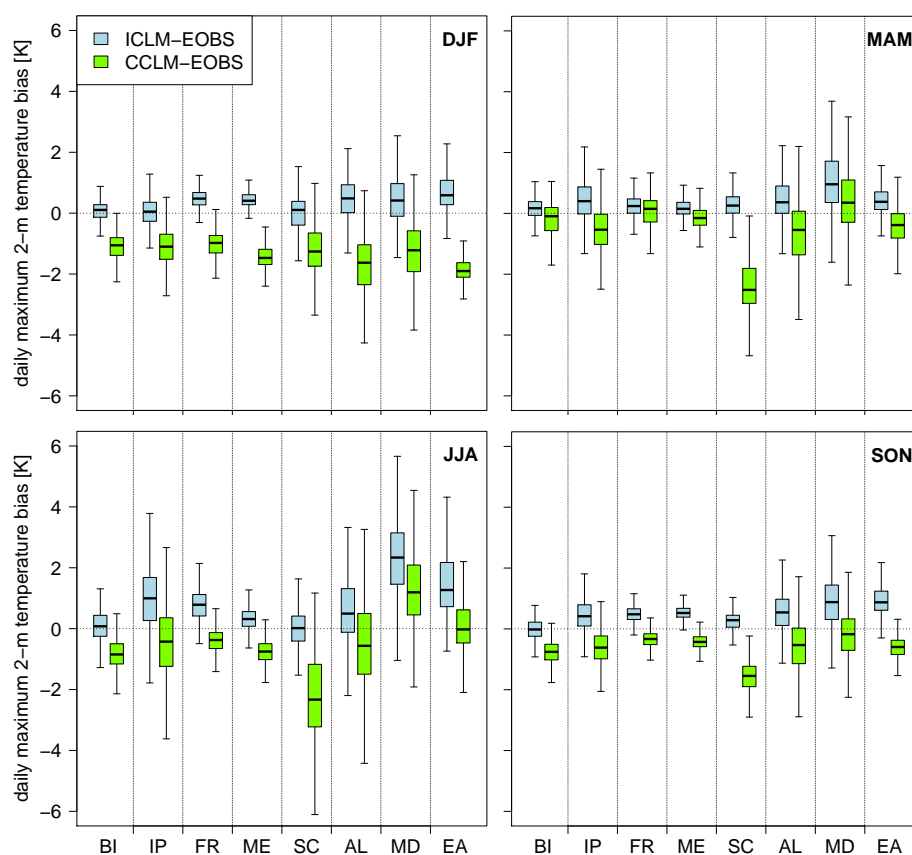**Figure 6.** Same as Figure 5 but for daily maximum 2-m temperature.
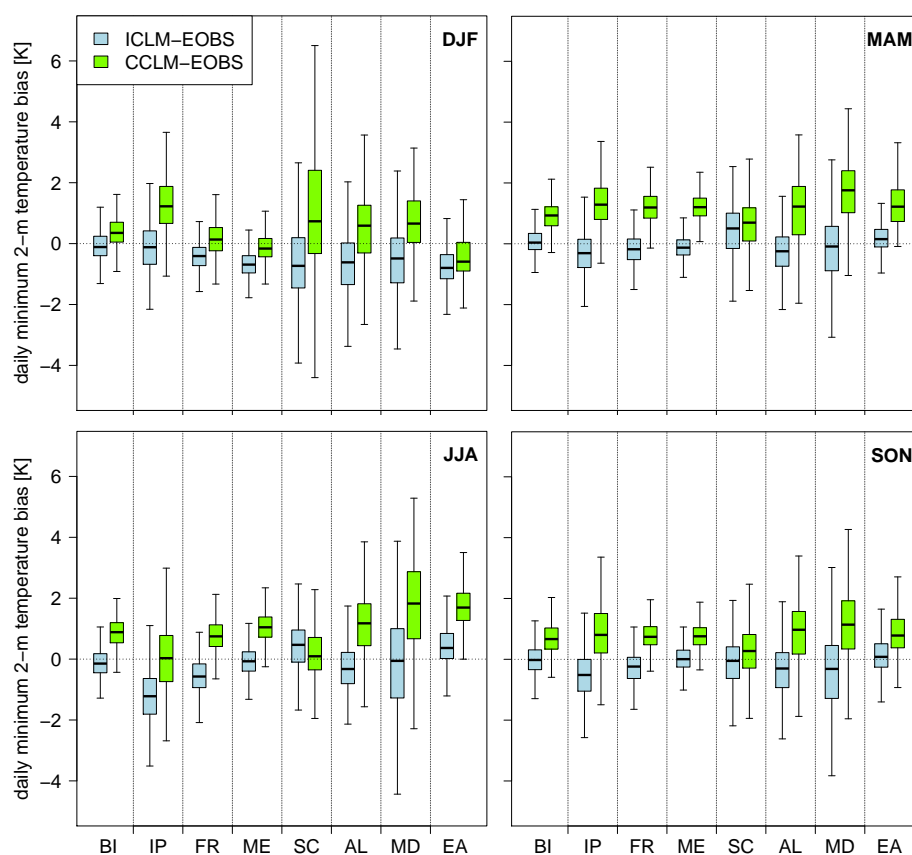
Figure 7. Same as Figure 5 but for daily minimum 2-m temperature.

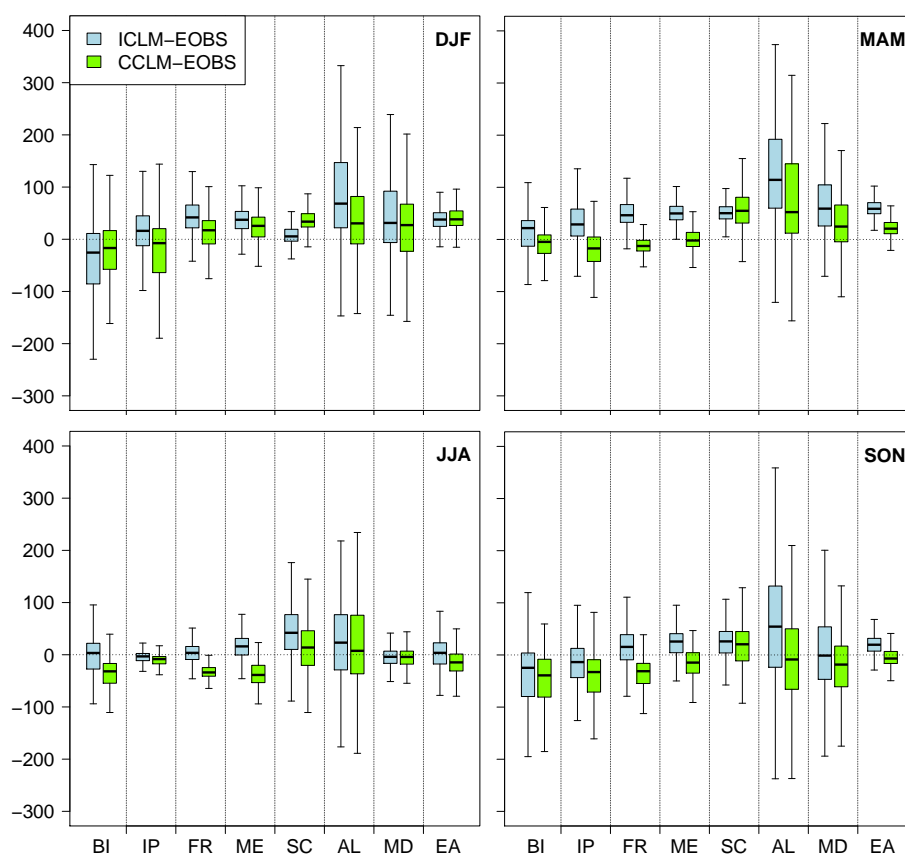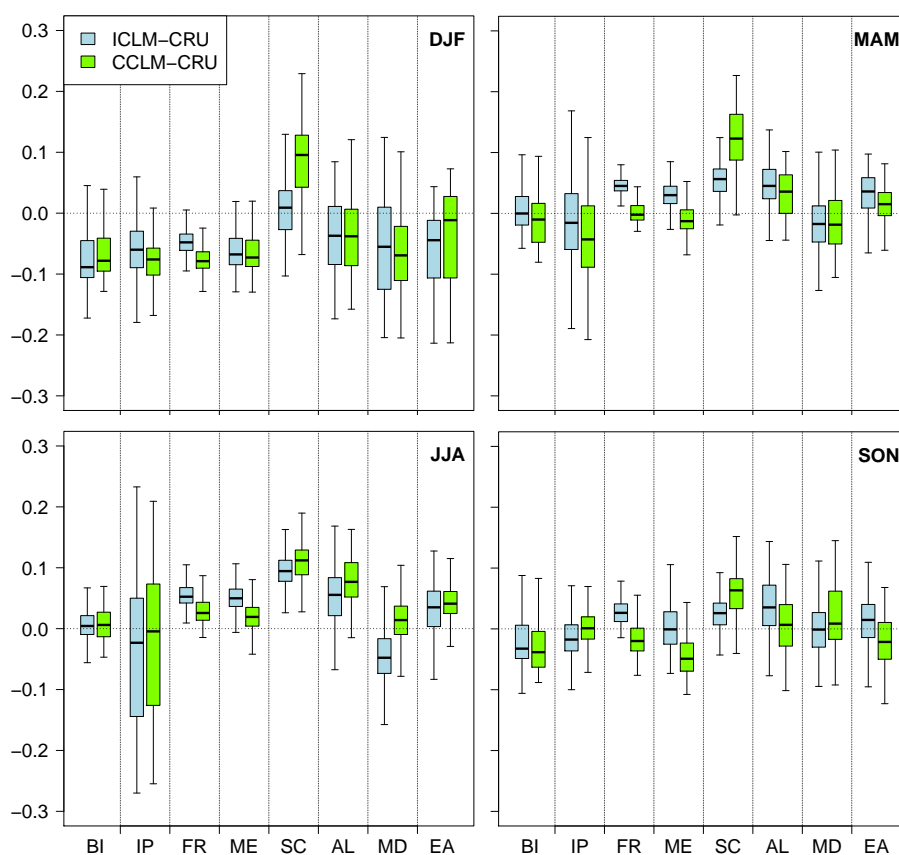**Figure 8.** Same as Figure 5 but for total precipitation.

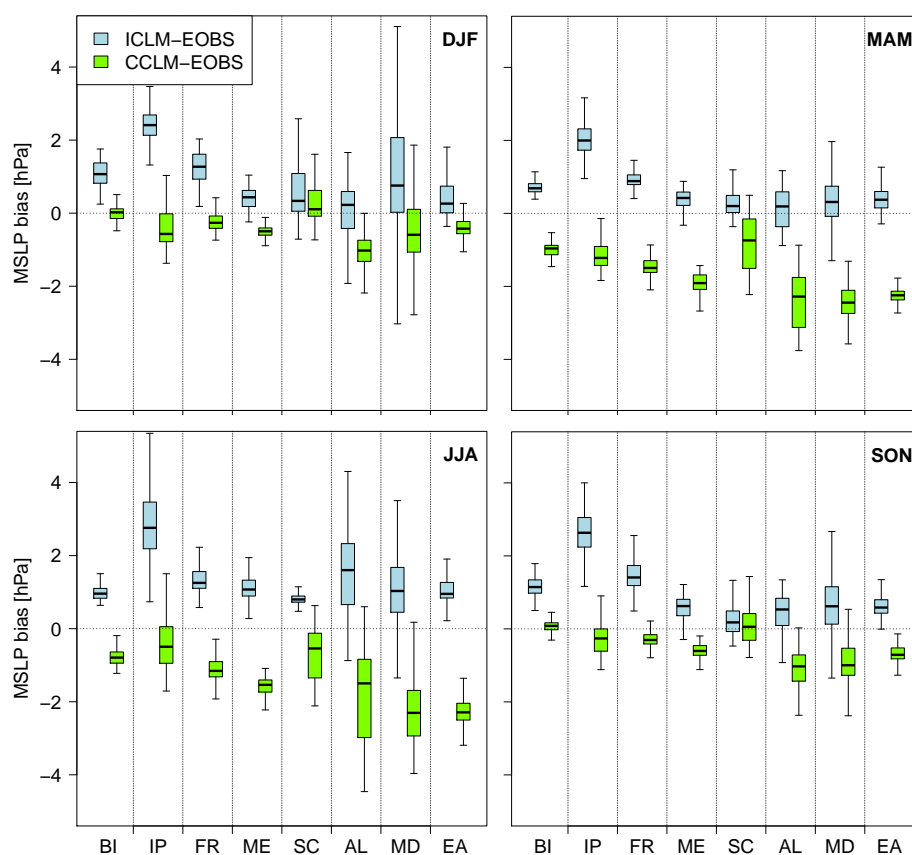**Figure 9.** Same as Figure 5 but for total cloud cover.
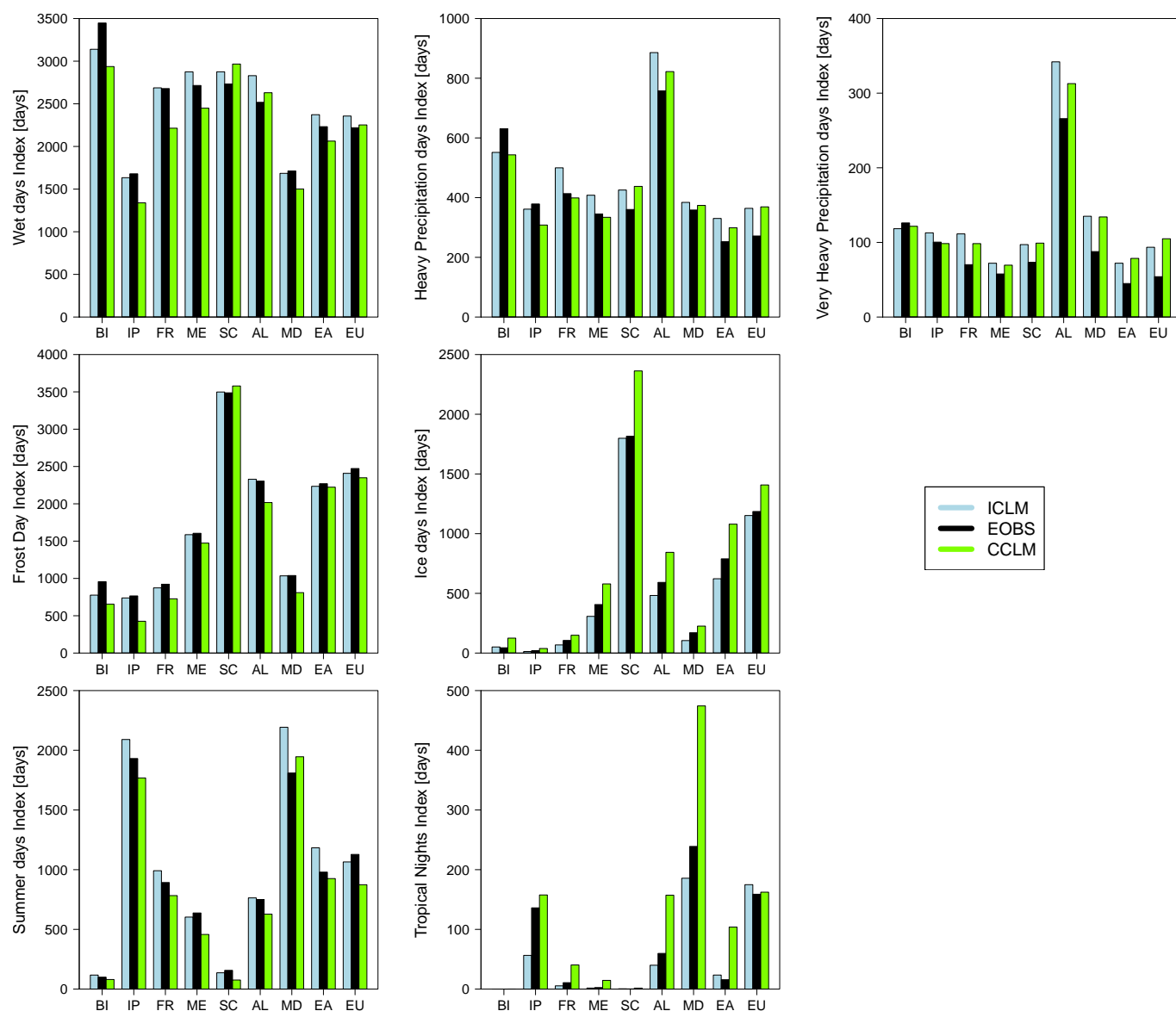
Figure 10. Same as Figure 5 but for MSLP.

Figure 11. Area mean of climate indices calculated from daily extreme air temperature and daily precipitation data of ICLM-REF, CCLM-REF and E-OBS for the PRUDENCE sub-regions and for the whole Europe (denoted EU) accumulated over the period 1981-2000.

Geoscientific
Model Development
Discussions

Table 1. Comparison between COSMO-CLM and ICON-CLM models.

	COSMO-CLM	ICON-CLM
Planetary boundary layer scheme	Prognostic turbulent kinetic energy closure Doms et al. (2011)	Wave dissipation at critical level Orr et al. (2010)
Cumulus convection scheme	Tiedtke (1989)	Mass flux shallow and deep Tiedtke (1989); Bechtold et al. (2008)
Cloud microphysic scheme	Seifert and Beheng (2001), reduced to one-moment scheme	Single-moment scheme Doms et al. (2011); Seifert and Beheng (2001)
Radiation scheme	Ritter and Geleyn (1992)	RRTM (Rapid Radiative Transfer Model) Mlawer et al. (1997); Barker et al. (2003)
Land surface and soil scheme	TERRA-ML Doms et al. (2011)	Tiled TERRA Schrodin and Heise (2001); Schulz et al. (2016)
Coordinate system	– horizontal: rotated geographical (lat/lon) – vertical: terrain following Gal-Chen height coordinate Gal-Chen and Somerville (1975) and exponential height coordinate (SLEVE) according to Schär et al. (2002)	– horizontal: icosahedral grids – vertical: terrain following Gal-Chen height coordinate Gal-Chen and Somerville (1975) and exponential height coordinate (SLEVE) according to Schär et al. (2002)

26

Table 2. Description of climate indices.

Index	Description	Unit
Frost days index	Number of days with minimum 2-m temperature $< 0^{\circ}$C	Days
Ice days index	Number of days with maximum 2-m temperature $< 0^{\circ}$C	Days
Summer days index	Number of days with maximum 2-m temperature $> 25^{\circ}$C	Days
Tropical nights index	Number of days with minimum 2-m temperature $> 20^{\circ}$C	Days
Wet days index	Number of days with total precipitation ≥ 1 mm	Days
Heavy precipitation days index	Number of days with total precipitation > 10 mm	Days
Very heavy precipitation days index	Number of days with total precipitation > 20 mm	Days

Geoscientific
Model Development
Discussions

Open Access

EGU

Table 3. RMSE and annual mean of spatial standard deviation of average monthly 2-m temperature for the PRUDENCE sub-regions. Data from ICLM-REF, CCLM-REF and E-OBS from 1981 to 2000.

	RMSE [K]		Standard deviation		
	ICLM	CCLM	ICLM	EOBS	CCLM
BI	0.34	0.39	4.37	4.41	4.58
IP	0.54	0.44	6.45	6.46	6.35
FR	0.53	0.56	5.71	5.74	5.95
ME	0.56	0.73	6.50	6.54	6.91
SC	0.60	0.76	8.76	8.72	8.40
AL	0.53	0.59	7.73	7.65	8.09
MD	0.65	0.87	7.67	7.47	7.86
EA	0.87	1.03	8.46	8.22	9.03

Table 4. Same as Table 3 but for maximum 2-m temperature.

	RMSE [K]		Standard deviation		
	ICLM	**CCLM**	**ICLM**	**EOBS**	**CCLM**
BI	0.42	0.88	5.05	4.98	5.17
IP	0.81	0.81	7.80	7.44	7.77
FR	0.86	0.77	6.79	6.66	6.87
ME	0.76	1.01	7.42	7.56	7.80
SC	0.58	1.91	9.15	9.18	8.94
AL	0.80	1.11	8.38	8.41	8.87
MD	1.54	1.08	8.86	8.19	9.06
EA	1.29	1.19	9.64	9.36	10.12

Geoscientific
Model Development
Discussions

Table 5. Same as Table 3 but for minimum 2-m temperature.

	RMSE [K]		Standard deviation		
	ICLM	CCLM	ICLM	EOBS	CCLM
BI	0.36	0.87	3.90	3.95	4.10
IP	0.81	1.15	5.28	5.69	5.13
FR	0.69	0.95	4.89	4.94	5.09
ME	0.72	1.05	5.93	5.68	6.08
SC	0.81	0.84	8.73	8.61	7.92
AL	0.75	1.06	7.33	6.97	7.49
MD	0.60	1.53	6.82	6.74	6.94
EA	0.85	1.38	7.68	7.21	8.02

Geoscientific
Model Development
Discussions

Table 6. Same as Table 3 but for total precipitation.

	RMSE [mm]		Standard deviation		
	ICLM	CCLM	ICLM	EOBS	CCLM
BI	0.55	0.52	1.79	2.10	1.80
IP	0.34	0.45	1.96	1.87	1.65
FR	0.57	0.44	1.55	1.35	1.40
ME	0.47	0.40	1.25	1.21	1.18
SC	0.48	0.49	1.94	1.70	1.81
AL	1.00	0.75	2.76	2.22	2.46
MD	0.56	0.40	1.92	1.48	1.74
EA	0.54	0.41	1.18	1.07	1.14

Table 7. Same as Table 3 but for MSLP.

	RMSE [hPa]		Standard deviation		
	ICLM	CCLM	ICLM	EOBS	CCLM
BI	1.60	0.91	6.11	5.92	5.95
IP	1.90	0.77	4.48	4.41	4.45
FR	1.71	1.12	4.74	4.47	4.73
ME	1.43	1.56	4.59	4.36	4.73
SC	1.21	0.91	6.20	6.21	6.09
AL	1.32	1.87	4.26	3.99	4.59
MD	1.68	1.79	3.84	3.67	4.29
EA	1.44	1.91	4.28	4.11	4.83